Initial Acquisition for MANET with Simultaneous Transmissions

Yi Jiang, Babak Daneshrad, and Gregory Pottie
Electrical Engineering Dept., UCLA, CA 90095
Email: yjiangee@ucla.edu, babak@ee.ucla.edu, pottie@ee.ucla.edu

***Abstract*— As the next generation mobile ad hoc network (MANET) evolves to allow for multiple simultaneous transmissions within one-hop for higher spectral efficiency, the interferences from the peer nodes will pose a challenge to the initial acquisition in the MANET. In this paper, we propose a maximum likelihood (ML) method of initial acquisition of the preamble sequences. Simulations show that this proposed method is robust against the interferences. We also propose to use a pair of Zadoff-Chu (Z-C) sequences as the preamble. By exploiting the unique structure of the Z-C sequences, we can estimate both timing and frequency offsets through two fast Fourier transforms (FFT). The estimation of the channel response and the interference covariance is also obtained as a by-product. Simulation results verified that the presented method is efficient in interference suppression and may allow for dozens of simultaneous transmissions.**

Keywords—MANET, maximum likelihood estimation, carrier frequency offset, synchronization

I. INTRODUCTION

The current standard multi-medium access (MAC) protocols for mobile ad hoc network (MANET), such as the carrier sense multiple access with collision avoidance (CSMA/CA), allows for only one active link while the nodes within one-hop of the transmitter should refrain from transmission [1][2]. But to achieve higher throughput given the limited frequency bandwidth, the next generation MANET will evolve to adopt a MAC for simultaneous transmission, such as the MAC design proposed in [3]. To establish a communication link, the receiver (Rx) node first needs to acquire the preamble sequence of transmitter (Tx) node and estimate the timing and frequency offset. While initial preamble acquisition is a classic and well-studied problem (see e.g., [4][5][6]), the interferences from the peer nodes due to simultaneous transmissions will pose a unique challenge which motivates a new study.

In this paper, we study this problem and propose a maximum likelihood (ML) based method for the estimation of the timing offset and carrier frequency offset (CFO). Moreover, we propose to use a pair of Zadoff-Chu sequences [7] as the preamble so that we can estimate the timing and frequency offset through two *one-dimensional* fast Fourier transforms (FFT). The estimation of the channel response and the interference covariance is also obtained as a by-product. The estimation of the channel response and the interference covariance are also obtained as a by-product.

In preparing this paper, we noticed paper [5] where the authors also proposed to use a pair of Zadoff-Chu sequences as the preamble. But our work in this paper differs in at least two aspects: first, we fully exploit the unique structure of the pair of Zadoff-Chu sequences so that we can estimate the two-dimensional timing and frequency offsets through two *one-dimensional* fast Fourier transforms (FFT); second, our work is motivated by MANET applications and emphasizes on the capability of suppressing interferences from the peer nodes.

The remainder of the paper is organized as follows. Section II presents the signal model. In Section III we derive an ML estimation of the timing offset and CFO of a channel for general preamble sequences. In Section IV we propose to use a pair of Zadoff-Chu sequence as the preamble and derive a surprisingly simple algorithm for both timing and frequency offset estimation using two FFTs. The simulation results are shown in Section V.

II. SIGNAL MODEL

We consider a frequency flathyembe SIMO (single-input multi-output) channel where the receiver has M Rx antennas. The received baseband signal can be represented as

$$\boldsymbol{x}_n = \boldsymbol{h}e^{j2\pi\Delta_f n}s_{n-\tau} + \boldsymbol{\nu}(n) \text{ for } n = 0, \dots, N-1 \qquad (1)$$

where $\boldsymbol{h} \in \mathbb{C}^M$ is the vector channel response, $\Delta_f \in (-0.5, 0.5)$ is the CFO normalized by the sampling frequency, and the preamble sequence $\{s_n\}_{n=0}^{N-1}$ is known but is subject to some unknown timing offset τ. $\boldsymbol{\nu}(n) \in \mathbb{C}^M$ is the lump sum of the interference plus noise, which is modeled as a zero-mean Gaussian vector with an unknown covariance matrix $\boldsymbol{Q}$. The power of the interference-plus-noise, measured by $\mathrm{Tr}(\boldsymbol{Q})$ can be much stronger than the received signal power $\mathbb{E}[|s_n|^2]$ due to the adjacent interferences.

The question is how a node can achieve initial acquisition reliably by completing the following tasks even in the presence of strong interferences

1. detecting the presence of the preamble sequence
2. estimating the timing offset τ of the preamble
3. estimating the frequency offset Δ_f

In this paper, we assume the presence of the signal and study the efficient and interference-robust algorithm to achieve the second and third tasks.

Although one can use the processing gain of a very long preamble sequence to suppress the interferences, it causes

large overhead and reduced bandwidth for data transmission. Instead, we use array processing to achieve interference suppression as explained in the next.

III. Optimum Estimation of Timing and Frequency Offset

First, let us assume for now that the received signal has been aligned with the local copy of the preamble sequence, i.e., the timing offset is known already. We derive the maximum likelihood estimation of the carrier frequency offset (CFO). The estimations of the channel response and the interference covariance are also obtained as by-product. The issue of the synchronization will be addressed later in this section.

From (1), we can derive the normalized log-likelihood function of $\{\boldsymbol{x}_n\}_{n=0}^{N-1}$ is

$$C = -\ln|\boldsymbol{Q}| - \mathrm{Tr}\left[\boldsymbol{Q}^{-1}\frac{1}{N}\sum_{n=0}^{N-1}(\boldsymbol{x}_n - \boldsymbol{h}e^{j2\pi\Delta_f n}s_n)(\boldsymbol{x}_n - \boldsymbol{h}e^{j2\pi\Delta_f n}s_n)^H\right]. \quad (2)$$

where $\boldsymbol{Q}$ is the covariance matrix of the interference-plus-noise. Maximizing the likelihood function (2) with respect to $\boldsymbol{Q}$ yields (see, e.g., [8] for the derivations)

$$\widehat{\boldsymbol{Q}}_{ML} = \frac{1}{N}\sum_{n=0}^{N-1}(\boldsymbol{x}_n - \boldsymbol{h}e^{j2\pi\Delta_f n}s_n)(\boldsymbol{x}_n - \boldsymbol{h}e^{j2\pi\Delta_f n}s_n)^H \quad (3)$$

Inserting (3) into (2) yields the ML estimation of Δ_f and $\boldsymbol{h}$ as

$$\widehat{\boldsymbol{h}}, \widehat{\Delta}_f = \arg\min_{\Delta_f}\left|\frac{1}{N}\sum_{n=0}^{N-1}(\boldsymbol{x}_n - \boldsymbol{h}e^{j2\pi\Delta_f n}s_n)(\boldsymbol{x}_n - \boldsymbol{h}e^{j2\pi\Delta_f n}s_n)^H\right|$$

$$= \arg\min_{\Delta_f}\left|\frac{1}{N}\sum_{n=0}^{N-1}(\boldsymbol{h}\boldsymbol{h}^H s_n s_n^* - 2Re\{\boldsymbol{x}_n e^{-j2\pi\Delta_f n}s_n^*\boldsymbol{h}^H\} + \boldsymbol{x}_n\boldsymbol{x}_n^H)\right|$$

Denoting

$$\boldsymbol{r}_{xs}(\Delta_f) \triangleq \frac{1}{N}\sum_{n=0}^{N-1}\boldsymbol{x}_n s_n^* e^{-j2\pi\Delta_f n} \quad (4)$$

$$\boldsymbol{R}_x = \frac{1}{N}\sum_{n=0}^{N-1}\boldsymbol{x}_n\boldsymbol{x}_n^H \quad (5)$$

and

$$P_s \triangleq \frac{1}{N}\sum_{n=0}^{N-1}s_n s_n^* \ \ (=1 \text{ w.l.o.g.}) \quad (6)$$

we obtain

$$\widehat{\boldsymbol{h}}, \hat{\Delta}_f = \arg\min_{\Delta_f}\left|\boldsymbol{R}_x - \boldsymbol{r}_{xs}(\Delta_f)\boldsymbol{r}_{xs}^H(\Delta_f) + \left(\boldsymbol{h} - \boldsymbol{r}_{xs}(\Delta_f)\right)P_s\left(\boldsymbol{h} - \boldsymbol{r}_{xs}(\Delta_f)\right)^H\right| \quad (7)$$

Since

$$\boldsymbol{R}_x - \frac{\boldsymbol{r}_{xs}(\Delta_f)\boldsymbol{r}_{xs}^H(\Delta_f)}{P_s} + \left(\boldsymbol{h} - \frac{\boldsymbol{r}_{xs}(\Delta_f)}{P_s}\right)P_s\left(\boldsymbol{h} - \frac{r_{xs}(\Delta_f)}{P_s}\right)^H \succcurlyeq \boldsymbol{R}_x - \frac{\boldsymbol{r}_{xs}(\Delta_f)\boldsymbol{r}_{xs}^H(\Delta_f)}{P_s}, \quad (8)$$

it follows that only when

$$\widehat{\boldsymbol{h}}_{\mathrm{ML}} = \boldsymbol{r}_{xs}(\Delta_f)$$

the determinant in (7) will be minimized. Therefore

$$\widehat{\Delta}_{f,\mathrm{ML}} = \arg\min_{\Delta_f}\left|\boldsymbol{R}_x - \boldsymbol{r}_{xs}(\Delta_f)\boldsymbol{r}_{xs}^H(\Delta_f)\right| \quad (9)$$

$$= \arg\min_{\Delta_f}|\boldsymbol{R}_x|\left|\boldsymbol{I} - \boldsymbol{R}_x^{-1}\left(\boldsymbol{r}_{xs}(\Delta_f)\boldsymbol{r}_{xs}^H(\Delta_f)\right)\right|, \quad (10)$$

$$= \arg\max_{\Delta_f}\boldsymbol{r}_{xs}^H(\Delta_f)\boldsymbol{R}_x^{-1}\boldsymbol{r}_{xs}(\Delta_f), \quad (11)$$

where to get (11) from (10), we used the property that $|\boldsymbol{I} + \boldsymbol{A}\boldsymbol{B}| = |\boldsymbol{I} + \boldsymbol{B}\boldsymbol{A}|$.

In summary, the ML estimates are

$$\widehat{\Delta}_{f,\mathrm{ML}} = \arg\max_{\Delta_f}\boldsymbol{r}_{xs}^H(\Delta_f)\boldsymbol{R}_x^{-1}\boldsymbol{r}_{xs}(\Delta_f) \quad (12)$$

$$\widehat{\boldsymbol{h}}_{\mathrm{ML}} = \boldsymbol{r}_{xs}(\Delta_{f,\mathrm{ML}}) \quad (13)$$

$$\widehat{\boldsymbol{Q}}_{ML} = \boldsymbol{R}_x - \boldsymbol{r}_{xs}(\Delta_f)\boldsymbol{r}_{xs}^H(\Delta_f) \quad (14)$$

From the above three equations, the frequency offset estimation (12) is the key. In the following, we give an efficient estimation method of the frequency offset.

A. Frequency Offset Estimation based on FFT

We first compute the M-vectors $\{\boldsymbol{x}_n s_n^*\}_{n=0}^{N-1}$ and form them into an $M \times N$ matrix denoted as $\widetilde{\boldsymbol{X}}$. Then apply an L-FFT along the time domain (i.e., the rows) of $\widetilde{\boldsymbol{X}}$ to obtain a new matrix $\boldsymbol{Y} \in \mathbb{C}^{M\times L}$, with column vectors $\{\boldsymbol{y}_l\}_{n=0}^{L-1}$. That is, the $(m,l)^{\text{th}}$ entry of $\boldsymbol{Y}$ is

$$y_{ml} = \sum_{n=0}^{N-1}\tilde{x}_{mn}\,e^{-\frac{j2\pi}{L}nl}.$$

We then compute the values,

$$p_l \triangleq \boldsymbol{y}_l^H\boldsymbol{R}_x^{-1}\boldsymbol{y}_l, \text{for } l = 0, \ldots, L-1 \quad (15)$$

where $\boldsymbol{R}_x$ is computed based on (5). Denote

$$i = \arg\max_l\{p_l, l = 0, \ldots, L-1\}. \quad (16)$$

Then

$$\hat{\Delta}_f = \begin{cases} \dfrac{i}{L} & 0 \le i \le \dfrac{L}{2} \\ \dfrac{i}{L} - 1 & \dfrac{L}{2} \le i \le L-1 \end{cases}$$

This estimation algorithm takes $O(ML\log_2 L + M^2 L)$ flops. Note that the absolute frequency offset is $\Delta_f \cdot f_s$, where f_s is the sampling rate.

We note that for the problem of interest, the CFO $\Delta_f \sim 0$, after being normalized by the Nyquist sampling. For instance, the CFO of the local oscillators (LO) of the Tx and Rx nodes is no greater than 40ppm according to the spec of IEEE 802.11. For central frequency 2.4GHz and CFO of 40ppm, the absolute CFO in Hz is no greater than 96KHz. Even if Nyquist sampling rate of 1.25MHz, $\Delta_f \le \frac{96\mathrm{KHz}}{1.25\mathrm{MHz}} = 0.077$. With this observation in mind, the computation of p_l in (15) and the

search in (16) can be limited to a small set of the indices around the zero frequency.

B. Timing Offset Estimation

In the study above, we have assumed that the synchronization is already achieved. But in practice, the timing offset estimation and frequency offset estimation are intertwined. In the following, we study the joint estimation of packet synchronization and CFO. Now introduce the uncertainty of the timing of the synchronization sequence, we define

$$\boldsymbol{r}_{xs}(\Delta_f,\tau) \triangleq \frac{1}{N}\sum_{n=0}^{N-1} \boldsymbol{x}_{n-\tau} s_n^* e^{-j2\pi\Delta_f n} \tag{17}$$

$$\boldsymbol{R}_x(\tau) = \frac{1}{N}\sum_{n=0}^{N-1} \boldsymbol{x}_{n-\tau}\boldsymbol{x}_{n-\tau}^H \tag{18}$$

which are similar to (4) and (5), respectively, except for the added parameter τ. It can easily seen from (12) that the MLE of the timing offset estimation and frequency offset would be

$$\hat{\Delta}_{f,\mathrm{ML}}, \hat{\tau} = \arg\max_{\Delta_f} \boldsymbol{r}_{xs}^H(\Delta_f,\tau)\boldsymbol{R}_x^{-1}(\tau)\boldsymbol{r}_{xs}(\Delta_f,\tau) \tag{19}$$

which requires a two-dimensional search.

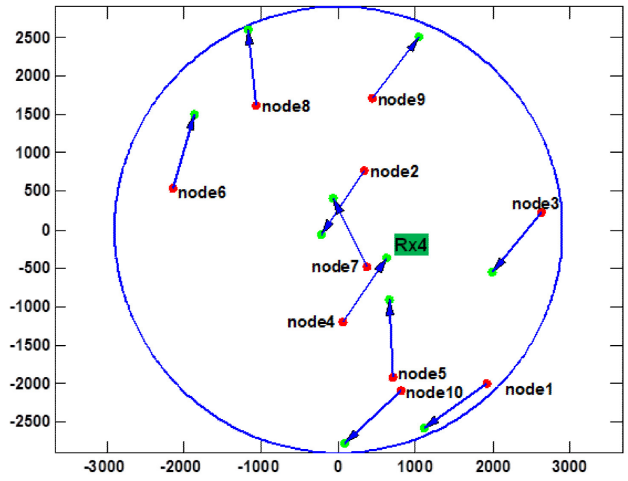

Figure 1 Topology of a 20-node (10 pairs of nodes) random network

The term $\boldsymbol{R}_x^{-1}$ in (19) is very important for interference suppression. To illustrate this point, we simulated a 20-node network where the nodes are located uniformly at random within a circle with radius 2900m, as shown in Figure 1. The 10 Tx-Rx pairs are indicated by the blue arrows, with Tx-Rx distance 1000m. Furthermore, we assume that all the 10 pairs of nodes were sending preambles simultaneously. Hence there are a lot of interferences between the peer nodes. In particular, note that Rx4 is very close to the transmitter node7, resulting input signal-to-interference ratio (SIR) less than -20dB. Assume that we use 1023-length Gold sequences as the preambles for each links. Figure 2 visualizes the two-dimensional function $\boldsymbol{r}_{xs}^H(\Delta_f,\tau)\boldsymbol{R}_x^{-1}(\tau)\boldsymbol{r}_{xs}(\Delta_f,\tau)$ (left) vs. $\boldsymbol{r}_{xs}^H(\Delta_f,\tau)\boldsymbol{r}_{xs}(\Delta_f,\tau)$ (right). From the left subplot, we can clearly identify a peak whose x-axis and y-axis indicate the timing and frequency offsets, respectively. However, the peak is not prominent in the right subplot due to not having the term $\boldsymbol{R}_x^{-1}$.

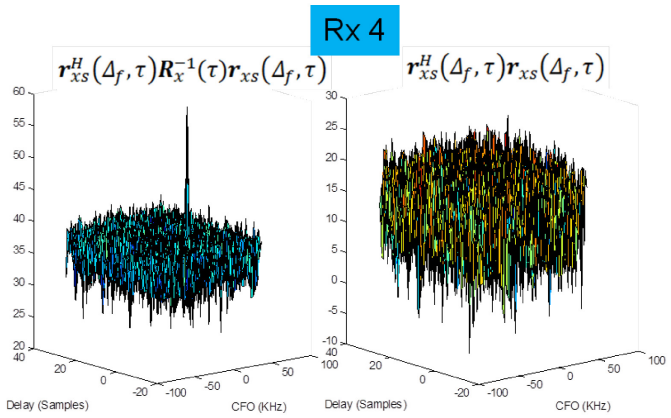

Figure 2 Two dimension function $\boldsymbol{r}_{xs}^H(\Delta_f,\tau)\boldsymbol{R}_x^{-1}(\tau)\boldsymbol{r}_{xs}(\Delta_f,\tau)$ (left) and $\boldsymbol{r}_{xs}^H(\Delta_f,\tau)\boldsymbol{r}_{xs}(\Delta_f,\tau)$ (right) based on Gold synchronization sequences

IV. Inital Synchronization based on Pairs Zadoff-Chu Sequences

The simulation example in the previous section indicates that to estimate the timing and frequency offset, we need to conduct a two-dimensional search to identify the peak. But we will show below that if use a pair of Zadoff-Chu (Z-C) sequences as the preamble, the timing and frequency offset estimation will be dramatically simplified.

Recall that a Z-C sequence of length N is [7]

$$\boldsymbol{s}_r = \left\{ s_r(n) = e^{\frac{j\pi r n(n+1)}{N}},\ n = 0,1,\ldots,N-1 \right\} \text{ if } N \text{ is odd} \tag{20}$$

where r should be co-prime with N. If there is a timing offset τ, then

$$s_r(n-\tau) = e^{\frac{j\pi r(n-\tau)(n+1-\tau)}{N}} = e^{\frac{j\pi r(-\tau+\tau^2)}{N}} e^{\frac{-j2\pi r\tau}{N}n} \cdot s_r(n) \tag{21}$$

where we can see that with delay τ, the received signal amounts to being linearly modulated by the phase $e^{-\frac{j2\pi r\tau}{N}n}$, or the original Z-C sequence with a frequency offset $\frac{2\pi r\tau}{N}$. On the other hand, if there is a frequency offset, it may appears to the receiver as a timing shift. Hence there is a timing offset versus frequency offset ambiguity. To illustrate this point, we run a simulation similar to that of Figure 2 except that here the preambles are based on Z-C sequences with length 1021. The two-dimensional function $\boldsymbol{r}_{xs}^H(\Delta_f,\tau)\boldsymbol{R}_x^{-1}(\tau)\boldsymbol{r}_{xs}(\Delta_f,\tau)$ is shown in Figure 3. The timing offset versus frequency offset ambiguity is illustrated as the "ridge" in Figure 3.

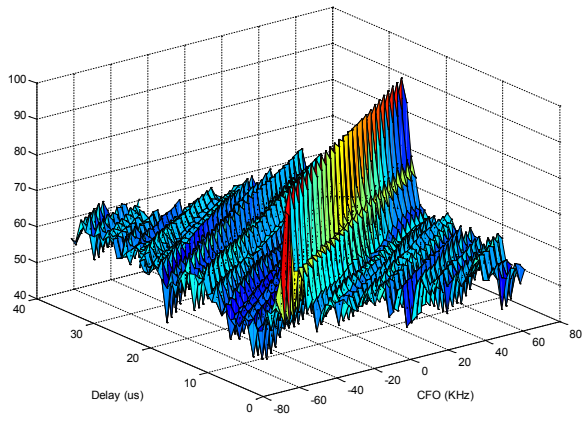

Figure 3 Two Dimension function $\boldsymbol{r_{xs}^H(\Delta_f,\tau)R_x^{-1}(\tau)r_{xs}(\Delta_f,\tau)}$ given Zadoff-Chu sequence based preamble.

This timing offset versus frequency offset ambiguity is actually desirable! The Rx node will not miss the ridge (and hence can more easily detect the presence of the sequence) by having a one-dimensional search along the time ignoring the frequency offset. More specifically, the node can compute

$$\boldsymbol{r}_{xs}(\tau) \triangleq \frac{1}{N}\sum_{n=0}^{N-1} \boldsymbol{x}_{n-\tau} s_r^*(n) \tag{22}$$

and the *one*-dimensional function $\boldsymbol{r_{xs}^H(\tau)R_x^{-1}(\tau)r_{xs}(\tau)}$. In contrast, if we use any other regular sequences as the preamble, such as Gold sequence used in the simulation for Figure 2, the peak is easy to miss if the frequency offset is not accurately estimated (and hence miss the presence of the sequence), which entails the much more complicated two-dimensional search, as illustrated by the left subplot of Figure 2.

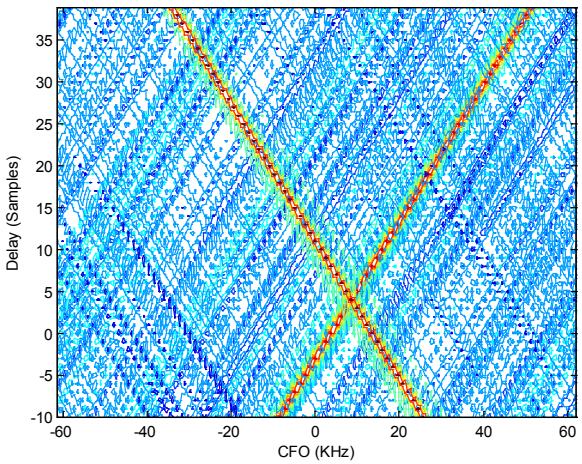

Figure 4 Contour of two dimensional function $\boldsymbol{r_{xs}^H(\Delta_f,\tau)R_x^{-1}(\tau)r_{xs}(\Delta_f,\tau)}$ based on preambles using pairs of Zadoff-Chu sequences.

To uniquely determine the timing offset and frequency offset, we propose to use a pair of Zadoff-Chu sequences $\boldsymbol{s}_r$ and $\boldsymbol{s}_{-r}$[1] for the joint estimation of the synchronization and frequency offset. That is, a transmitter will send a pair of Z-C sequences

$$\boldsymbol{s}_r \text{ and } \boldsymbol{s}_{-r}$$

simultaneously. If there are more than one Tx antennas, the two sequences will be sent from different antennas. Then there are two "ridges" in the two-dimension function $\boldsymbol{r_{xs}^H(\Delta_f,\tau)R_x^{-1}(\tau)r_{xs}(\Delta_f,\tau)}$. Figure 4 shows the contour of $\boldsymbol{r_{xs}^H(\Delta_f,\tau)R_x^{-1}(\tau)r_{xs}(\Delta_f,\tau)}$ based on preambles using pairs of Zadoff-Chu sequences. The two straight red-yellowish lines correspond to the two "ridges", which cross at the location of (timing offset, frequency off)!

A. Estimates of Timing and Frequency Offset

The estimates of timing and frequency offset are derived as follows.

Similar to (21), given a synchronization offset τ, the delayed Zadoff-Chu sequence

$$s_{-r}(n-\tau) = e^{\frac{j\pi(-r)(-\tau+\tau^2)}{N}} e^{\frac{j2\pi r\tau}{N}n} \cdot s_{-r}(n) \tag{23}$$

For illustration purposes, let us ignore the noise and assume that the channel gain is one except for the CFO Δ_f. Then the received signal is

$$x_n = s_r(n-\tau)e^{j2\pi\Delta_f n} + s_{-r}(n-\tau)e^{j2\pi\Delta_f n},\ n = 0,1,\dots,N-1$$

Multiplying x_n element-wise by $s_r^*(n)$, we obtain

$$\begin{aligned} x_n s_r^*(n) = e^{\frac{j\pi r(-\tau+\tau^2)}{N}} e^{j2\pi\Delta_f n} e^{\frac{-j2\pi r\tau}{N}n} \\ + s_{-r}(n-\tau)s_r^*(n)e^{j2\pi\Delta_f n}, \\ n = 0,1,\dots,N-1 \end{aligned} \tag{24}$$

where the first term is a sinusoid with frequency $\Delta_f - \frac{r\tau}{N}$. Applying an N-point FFT to the above sequence (24), we can estimate the frequency $\Delta_f - \frac{r\tau}{N}$ as the peak location of the FFT spectrum, which is denoted as

$$a = \Delta_f - \frac{r\tau}{N} \tag{25}$$

Note that the cross term $s_{-r}(n-\tau)s_r^*(n)$ in (24) is also a Zadoff-Chu sequence and therefore its FFT will show no peak. On the other hand, multiplying x_n element-wise by $s_{-r}^*(n)$, we obtain

$$\begin{aligned} x_n s_{-r}^*(n) = e^{\frac{j\pi(-r)(-\tau+\tau^2)}{N}} e^{j2\pi\Delta_f n} e^{\frac{j2\pi r\tau}{N}n} \\ + s_r(n-\tau)s_{-r}^*(n)e^{j2\pi\Delta_f n}, \\ n = 0,1,\dots,N-1, \end{aligned} \tag{26}$$

where the first term is a sinusoid with frequency $\Delta_f + \frac{r\tau}{N}$ Applying an N-point FFT to the sequence (26), we can estimate the frequency $\Delta_f + \frac{r\tau}{N}$ as the peak location of the FFT spectrum, which is denoted as

$$b = \Delta_f + \frac{r\tau}{N} \tag{27}$$

[1] Note that $\boldsymbol{s}_{-r}$ is equivalent to $\boldsymbol{s}_{N-r}$ as $e^{\frac{j\pi(N-r)n(n+1)}{N}} = e^{\frac{j\pi(-r)n(n+1)}{N}}$ for any integer number n.

As an example, Figure 5 shows the two overlapped FFT spectrums obtained by applying FFT to the sequences (24) and (26). The x-axis is the frequency normalized by the sampling rate. The location of the peaks are denoted as "a" and "b". Combining (25) and (27), we obtain that the estimation of the frequency offset is

$$\widehat{\Delta_f} = \frac{a+b}{2} \tag{28}$$

and the estimate of the timing offset is

$$\hat{\tau} = \frac{(b-a)N}{2r} \tag{29}$$

Thus no two-dimensional search is needed.

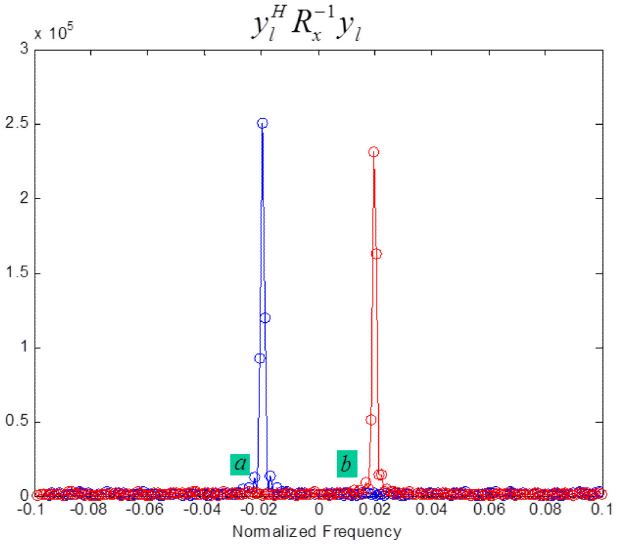

Figure 5 The two FFT spectrums obtained by applying FFT to the sequences (24) and (26).

To summarize, the procedure of timing and frequency offset estimation is as follows.

1. Given the received N vector samples $\{\boldsymbol{x}_n, n = 0, \dots, N-1\}$, wherein the preamble has some unknown delay, compute the covariance matrix
$$\boldsymbol{R}_x = \frac{1}{N}\sum_{n=0}^{N-1} \boldsymbol{x}_n \boldsymbol{x}_n^H$$
2. Apply element-wise multiplication of $s_r^*(n)$ and $\boldsymbol{x}_n$ to obtain an $M \times N$ matrix $\widetilde{\boldsymbol{X}}$ where the n th column $\widetilde{\boldsymbol{x}}_n = \boldsymbol{x}_n s_r^*(n)$.
3. Applying an L-point FFT ($L \geq N$) to each row of $\widetilde{\boldsymbol{X}}$, we obtain a $\boldsymbol{Y} \in \mathbb{C}^{M \times L}$ with columns $\boldsymbol{y}_l$'s.
4. For the frequency points of interest, compute $\boldsymbol{y}_l \boldsymbol{R}_x \boldsymbol{y}_l^{-1}$ and identify the index of the peak as l. If $l \geq L/2$, $l \leftarrow l - \frac{L}{2}$. Obtain $a = l/L$
5. To obtain b, repeat Step 2-4 but replace $\widetilde{\boldsymbol{x}}_n$ by $\widetilde{\boldsymbol{x}}_n = \boldsymbol{x}_n s_{-r}^*(n)$.
6. Given a and b, use (28) and (29) to estimate the frequency and timing offset, respectively.

B. Discussions

To further illustrate the proposed method, we give a plot as shown in Figure 6. The x-axis represents the frequency offset and the y-axis is the timing offset. For a pair of Zadoff-Chu sequences $s_r(n)$ and $s_{N-r}(n)$, the timing offset versus frequency offset ambiguity "ridges" correspond to the two straight lines with slop $\frac{r}{N}$ and $\frac{-r}{N}$, respectively. The two lines cross the x-axis at $(a, 0)$ and $(b, 0)$, and they cross each other at

$$\left(\frac{a+b}{2}, \frac{(b-a)N}{2r}\right) = (\widehat{\Delta_f}, \hat{\tau}).$$

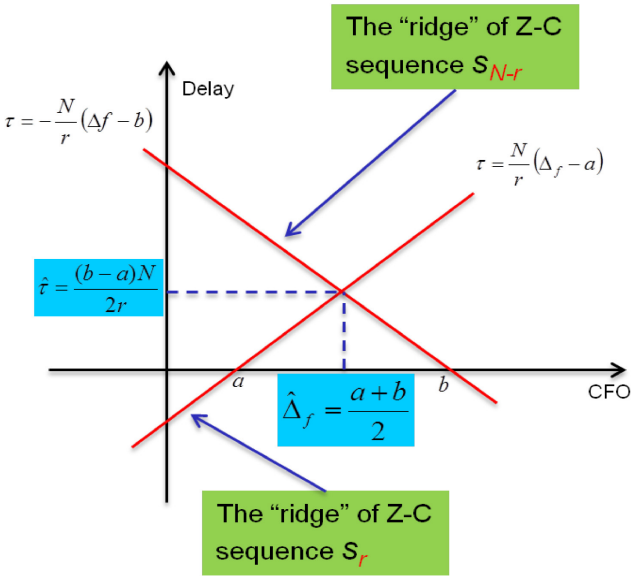

Figure 6 Illustration of the two "ridges" of Zadoff-Chu sequences and the location of the cross point.

We conclude this section by noting that while a Tx node use a pair of Zadoff-Chu sequence $\{\boldsymbol{s}_r, \boldsymbol{s}_{-r}\}$, different nodes use different parameter r, which is co-prime with N. In the simulations, we choose N to be prime so that any $r < N$ is coprime to N.

V. SIMULATION RESULTS

In this section, we present two simulations results to verify the effectiveness of our proposed method. The simulation setting is given in the table below. As shown in Figure 1, the nodes of the MANET are randomly distributed in a circle with radius 2.9Km.

Table 1 Simulation Setting

Central Frequency	1.3GHz
Bandwidth	1.25MHz
Circle Radius	2900m
Tx-Rx Distance	500, 1000, 1500, 2000m
Tx Power	40dBm
Antenna Gain	2dBi
Noise Figure	3dB
Pathloss Coefficient	3
LO Drift	10ppm (≤13KHz)
Number of Antennas per Node	$M = 4$

We also assume that the MANET has a synchronous MAC which regulates the nodes to transmit the preambles (pairs of Zadoff-Chu sequences) to their respective receivers about the same time up to some propagation delays (see e.g. the MAC design in [3]). Different nodes use the sequence pairs $\{\boldsymbol{s}_r, \boldsymbol{s}_{-r}\}$ but with different parameter r.

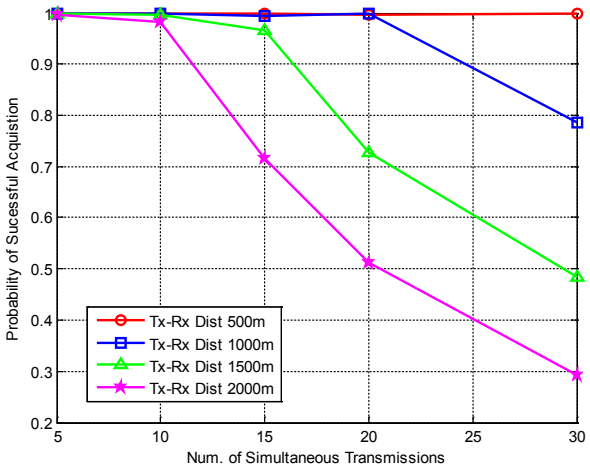

Figure 7 The probability of successful acquisition with different numbers of simultaneous transmission. The preambles are based on Z-C sequences with length 1021.

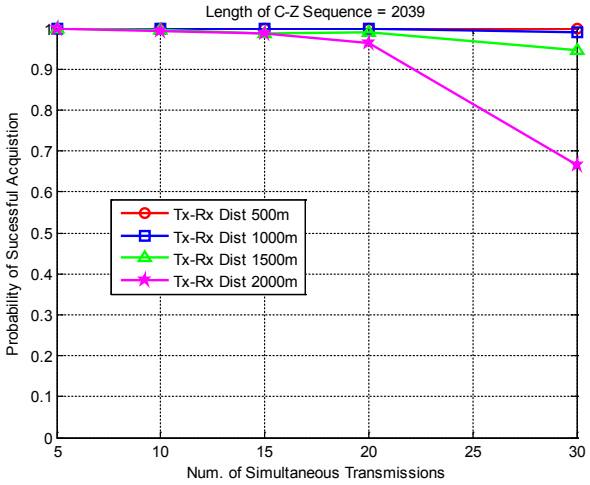

Figure 8 The probability of successful acquisition with different numbers of simultaneous transmission. The preambles are based on Z-C sequences with length 2039.

We simulated MANET where 5, 10, 20, and 30 nodes were making simultaneous transmission of the preamble sequences. We apply the timing and frequency offset estimation algorithm as detailed in Section IV for all the Rx nodes. If the error of time offset estimation $\leq$ Ts/4 *and* the error of frequency offset estimation $\leq$ 500Hz, then we regard it as a successful acquisition. We run Monte Carlo trials to see how the probability of successful acquisition varies with respect to different number of nodes, and the Tx-Rx distance. Figure 7 shows that in the case where the length of the Zadoff-Chu sequences is set to be 1021, for Tx-Rx distance of 500m, we can get 100% success rate of initial acquisition even when the number of nodes increases to 30. As the Tx-Rx distance increases, the interference from the peer nodes increases, which accounts for the reduced success rate. But even for Tx-Rx distance of 1500m and 15 simultaneous transmissions, the success is close to 100%, which allows for nearly 15 simultaneous transmissions in the MANET.

The simulation setting of Figure 8 is similar to that of Figure 7 except that the length of Zadoff-Chu sequences is nearly doubled to 2039.

VI. Conclusions

In this paper, we studied system initial synchronization for mobile ad hoc network (MANET) with simultaneous transmission. We first derived the maximum likelihood (ML) estimation of the timing and frequency offset of a received preamble sequences. But this ML method requires two-dimensional search over both time and frequency domains. We then proposed to use a pair of Zadoff-Chu sequences as the preamble so that we can estimate both timing and frequency offset simply through two fast Fourier transforms (FFT). Simulations show that this proposed method is robust against interferences from the concurrent peer.

VII. Acknowledgement

This work presented in this paper was funded by ONR Award No. N00014-14- 1-0104 : P00002

Reference

[1] IEEE 802.11: Wireless LAN Medium Access Control (MAC) and Physical Layer (PHY) Specifications

[2] H. Menouar, F. Filali, and M. Lenardi, "A Survey and Qualitative Analysis of MAC Protocols For Vehicular Ad Hoc Networks", *IEEE Wireless Commun,* vol. 14, No. 5, Oct. 2006, pp. 30 - 35

[3] Y. Jiang, H. Wang, B. Daneshrad, and B. Fette, "PHY and MAC design for distributed Tx-Rx beamforming in Mobile Ad Hoc Networks", *IEEE Military Communications Conference* (MILCOM), 2014, pp. 885-890.

[4] H. Minn, V. Bhargava, and K. Letaief, "A robust timing and frequency synchronization for OFDM systems," *IEEE Trans. Wireless Commun.*, vol. 2, no. 4, pp. 822–839, Jul. 2003.

[5] A. Coulson, "Maximum likelihood synchronization for OFDM using a pilot symbol: Algorithms," *IEEE J. Sel. Areas Commun.*, vol. 19, no. 12, pp. 2486–2494, Dec. 2001.

[6] G. M. M. U. Gul, X. Ma, and S. Lee, "Timing and frequency synchronization for OFDM downlink transmissions using Zadoff-Chu sequences," IEEE Trans. on Wireless Comm., Vol. 14, No. 3, pp. 1716-1729, March 2015

[7] D. C. Chu, "Polyphase codes with good periodic correlation properties", *IEEE Trans. Inform. Theory*, pp 531-533, 1972.

[8] A. L. Swindlehurst and P. Stoica, "Maximum likelihood methods in radar array signal processing," Proc. IEEE, vol. 86, pp. 421–441, Feb. 1998